Guided Waves Damage Identification in Beams with Test Pattern Dependent Series Neural Network Systems

C. K. LIEW, M. VEIDT
Division of Mechanical Engineering
University of Queensland
Brisbane, Qld 4072
AUSTRALIA
c.liew@uq.edu.au m.veidt@uq.edu.au

Abstract: - In regression neural networks for pattern recognition of preprocessed guided waves signals in beams, a trained network produced large errors when identifying a test pattern not found in the training set. To improve the accuracy of results, a new neural network procedure was introduced where progressive training was performed in a series combined network with the integration of a weight-range selection (WRS) technique that was dependent on the test pattern. The WRS method was applied for a supervised multi-layer perceptron operating with one hidden layer of neurons and trained using a backpropagation algorithm. The system was able to achieve average predictions accurate to 2.5% and 7.8% of the original training range sizes for the damage location and depth respectively while the WRS provided up to 13.9% improvement compared to equivalent conventional neural networks.

Key-Words: - pattern recognition, combined neural networks, generalization, ultrasonic guided waves, quantitative nondestructive evaluation, structural health monitoring

1 Introduction

Structural health monitoring is a field that aims to evaluate the integrity and safety of structures mainly for aerospace, civil and marine applications. The advent of advanced sensor technologies, accurate measuring instruments and the improvement in signal processing techniques have motivated the research and development of practical solutions to quantify damages in structures [1]. A technology that has gained much interest in the recent years are ultrasonic guided waves, which are highly sensitive in detecting discontinuities in their paths of propagation [2, 3]. However, identifying damages accurately from the measured transient wave response alone can prove difficult when a reasonably large damage parameter space is considered. Signal processing thus becomes an essential intermediate procedure in guided waves damage identification, leading to the application of pattern recognition with neural networks.

Pattern recognition with regression neural networks has recently been developed for guided waves signals to quantify damages in metal and composite structures [4, 5, 6]. These systems require the simulation of patterns with known damage parameters for the supervised neural network training as a practical and cost-effective approach. Simulations of wave responses from the given damage parameters can be calculated from considerations of the reflection and transmission coefficients at the damage boundaries [7] or by finite-element methods [8].

Although these simulations predict the wave response to adequate accuracies, there are some areas where experimental measurements will normally differ. These differences are sufficient to cause networks trained with simulated patterns to encounter difficulties in identifying experimental patterns. Discrepancies can originate from noise, pulse interference, mode coupling, dispersion and additional wave modes, all of which are difficult to predict and hence, not easy to reproduce in simulation. The occurrences of these effects are mostly case-specific, i.e. to the test pattern being identified. Hence, there must be an integral step to consider the test pattern during neural network training to obtain more accurate damage identification results. This motivates the research to develop a progressive training process through a series network that considers the intermediate test results from recognizing the test pattern.

In the next Section 2, the pattern recognition system is presented, outlining the experimental setup, simulation model, preprocessing procedure to obtain the inputs patterns, as well as the neural network architecture and design. The potential and the methodology of the test pattern dependent system are described in Section 3. The damage

identification results from the system are presented and discussed in Section 4 followed by a conclusion in Section 5.

2 Pattern Recognition for Guided Waves Damage Identification in Beams

A pattern recognition system was designed for a damage identification tool in beams investigated with guided waves. Single thin laminar damages were quantified in beams, which are elementary members of frames and trusses in structures.

Test patterns were obtained from measurements of the transient wave responses on beams fabricated with artificial laminar damages. On the other hand, training patterns were generated from a simulation based on the fundamental principles of wave propagation, reflection and transmission. Both patterns were preprocessed using the discrete wavelet transform, improving correlation between experimental and simulated patterns while reducing the neural network processing time.

A multi-layer perceptron feedforward neural network architecture trained with simulated patterns through a backpropagation algorithm was then used to identify the experimental test pattern. Further details of the input data acquisition procedures and the pattern recognition system are described in the following sections.

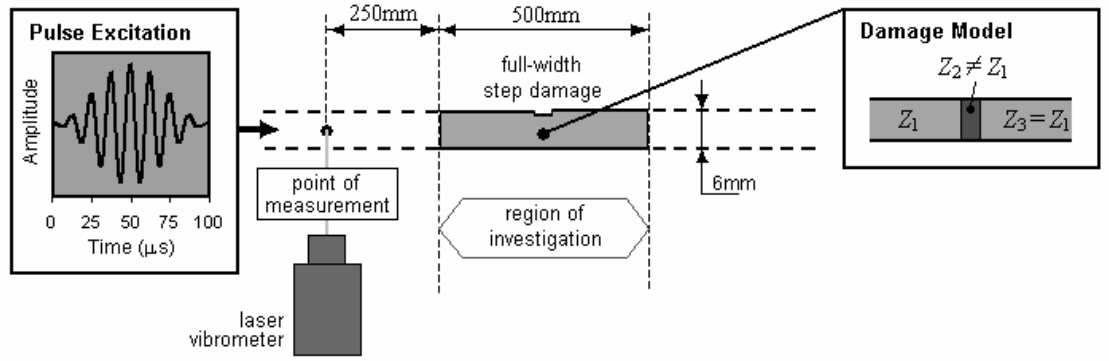

Fig. 1. 500mm region of investigation at the center of a beam specimen fabricated with a full-width step damage. Pulse Excitation inset shows the 8-cycle 80kHz Hanning windowed tone burst pulse as the interrogating wave while the Damage Model inset shows the inhomogeneity model for simulating training patterns.

2.1 Experiment

Aluminum beam specimens of 2 metres in length with rectangular cross-sections 12mm × 6mm were considered. A 2mm × 12mm × 6mm longitudinal Pz27 piezoceramic transducer was adhesively bonded to one end of the beam to excite an interrogating wave pulse into the beam. The transducer was wired to a SRS DS345 function generator to produce an 8-cycle 80kHz Hanning windowed tone burst pulse excitation, as depicted in the Pulse Excitation inset of Fig. 1. A Krohn-Hite 7500 amplifier was connected between the function generator and the transducer to increase the amplitude of the signal. Additionally, for a better signal-to-noise ratio response, a 4mm × 12mm × 6mm brass backing mass was adhesively bonded to the transducer. A Polytec OFV 303/OFV 3001 laser vibrometer system was used to measure the transient wave response at the center of the 6mm thickness surface of the beam. Measurements were collected at 500mm from the transducer-beam interface to obtain optimum separation among pulses and thus ensure minimum pulse interferences in the signal. Out-of-plane displacements were measured against time, which was displayed on a digital oscilloscope and transferred to a personal computer for storage and processing.

A full-width step damage was machined in a region of investigation located at the center of each beam, as shown in Fig. 1. This 500mm long region was taken as the original damage parameter space. Five beams were prepared and labeled according to the fabricated damages described in Table 1. Three damage parameters would be identified by pattern recognition, namely damage center location (DCP), damage depth (DD) and damage length (DL). Note that DCP was measured from the transducer-beam interface.

Table 1. Damage parameters fabricated on five test beams T1 – T5.

Beam	DCP (mm)	DD (mm)	DL (mm)
T1	820	2.5	25.0
T2	960	1.0	90.0
T3	1100	2.0	75.0
T4	1130	1.5	65.5
T5	1200	2.5	50.5

2.2 Simulation

The longitudinal wave velocity, c, was used to determine the arrival times of wave pulses at the point of measurement during simulation. c was approximated to travel at 4750m/s by comparing the change in incident pulse arrival times measured experimentally at several locations along the length of the beam. Note that this velocity was lower than theoretical group velocities in aluminum rods due to the complex dispersion in rectangular beams that cannot be quantified through an exact solution [9].

At the damage region, the wave was split into reflected and transmitted waves. The proportion of reflection and transmission were quantified by modeling the damage region as an inhomogeneity [7], described graphically in the Damage Model inset of Fig. 1. The inhomogeneity took on the same length as the damage with an equal cross-sectional area as the undamaged aluminum beam. However, the inhomogeneity region contained a different acoustic wave impedance, Z, compared to the aluminium beam. Z is an acousto-ultrasonic material property, as defined in Eq. (1) where ρ is the material density, c is the wave velocity, and A is the cross-sectional area of the specimen.

$$Z = \rho\, c\, A \tag{1}$$

For the step damage, there was a change in Z due to a change in A, which was a function of the beam thickness. Reflection and transmission coefficients at the boundaries of the damage region, C_R and C_T respectively, can thus be derived from Eq. (2) [10] where subscripts a and b denote the locations before and after a damage boundary.

$$C_R = \frac{Z_b - Z_a}{Z_a + Z_b}\ ,\ C_T = \frac{2Z_b}{Z_a + Z_b} \tag{2}$$

Signals of the transient wave response at the point of measurement for different damage parameters could then be generated by simulation based on the known c, C_R and C_T values. Training data was simulated randomly within the selected original parameter spaces at accuracies given in Table 2.

Table 2. Original damage parameter spaces and accuracies for simulation of training data.

Damage Parameter	Original Parameter Space (mm)	Accuracy (mm)
DCP	750 - 1250	1
DD	0 - 3.0	0.1
DL	0 - 100.0	0.1

2.3 Experimental and Simulated Signals

Fig. 2(a) shows an example of the extracted transient wave response signal for test beam T3 acquired from the point of measurement. The equivalent simulated signal based on the inhomogeneity model is also plotted. Both signals are normalized by the amplitude of the incident wave and the notable pulses are described. The arrival times of all the pulses can be easily checked from simple calculations with the known wave velocity and the distance traveled along the beam.

Signals within the 100μs-940μs range contained rich information regarding the damage and were extracted as neural network input. This range spanned from the incident wave to the first transmitted wave. The first transmitted wave was defined for a pulse that had traveled past the damage, reflected from the free end of the beam, and transmitted again through the damage before being collected at the point of measurement. Signals out of this range were not considered because there was only noise prior to 100μs while beyond 940μs the wave response was affected by the presence of severe attenuation and dispersion [10], which were features not included in the simulation.

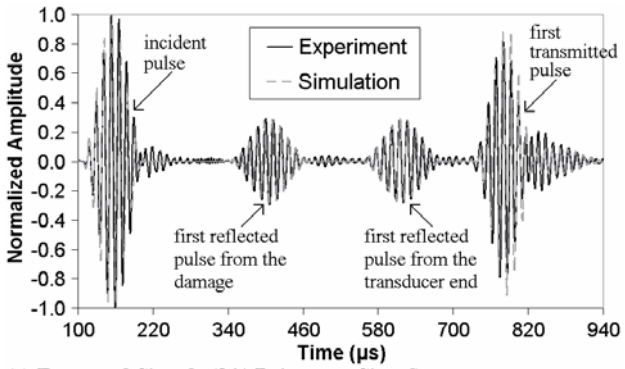

(a) Extracted Signals (841 Points per Signal)

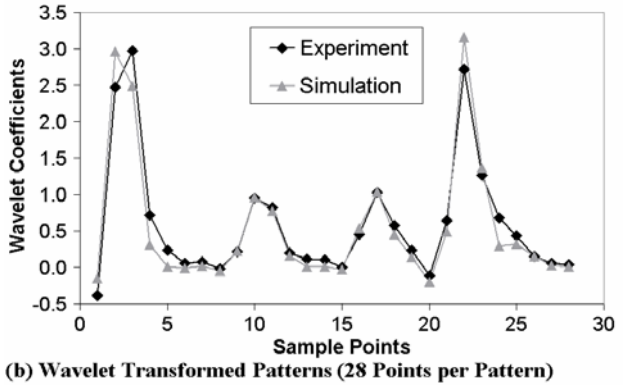

(b) Wavelet Transformed Patterns (28 Points per Pattern)

Fig. 2. Experimental and simulated extracted signals with corresponding preprocessed wavelet patterns for test beam specimen T3.

Table 3. Correlation coefficients between experimental and simulated extracted signals and wavelet patterns for the test beams.

Beam	T1	T2	T3	T4	T5
r_{sig}	0.132	0.115	0.299	0.174	0.285
r_{wav}	0.972	0.982	0.974	0.976	0.981

With low noise levels achieved with the laser vibrometer system, a generally good match with respect to pulse amplitudes and arrival times is observed between experimental and simulated signals, as evident in Fig. 2(a). However, weak correlation coefficients are calculated between extracted experimental and simulated signals, r_{sig}, as shown in Table 3.

As the pulse amplitudes and arrival times corresponded reasonably well between experiment and simulation, the weak r_{sig} values are mainly the result of inconsistent differences in the phase. These phase discrepancies are attributed to the complex dispersive behaviours of waves propagating in rectangular beams [9]. These properties can only be approximated with limited accuracies through elaborate numerical methods [11] and hence, are not feasible to produce training patterns.

2.4 Wavelet Transform Preprocessing

Discrepancies in the phase could lead to errors in pattern recognition, hence, preprocessing was performed to minimize these effects and to extract only important features from the signals. The discrete wavelet transform was applied, which decomposed the signal by reducing the number of sampling points through a wavelet derived filter bank in dyadic scales [4].

The absolute signals were transformed to produce wavelet patterns, as shown in Fig. 2(b). These wavelet patterns were the result of 5 levels of decomposition with the 8th order Daubechies wavelet. 5 levels of decomposition gave an optimum balance between resolution and downsampling while the 8th order Daucbechies wavelet was selected for its high regularity to locate local properties within the signal [12]. Essential features that described the damage viz. the pulse arrival times, magnitudes and lengths, were relatively preserved in the wavelet patterns.

The discrete wavelet transform increased the correlation coefficient between experimental and simulated patterns, r_{wav}, as evident in Table 3, which could improve the pattern recognition performance. In addition, the number of points was also reduced from 841 points at a sampling rate of 1MHz in an extracted signal to 28 points in a wavelet pattern. The shorter wavelet pattern thus provided the advantage of faster processing times when learning the simulated patterns during neural network training.

2.5 Neural Network Architecture and Design

The multi-layer perceptron feedforward neural network with a single hidden layer of neurons [13] was architecture selected for pattern recognition. This neural network contained a hyperbolic sigmoid activation function, F, to account for nonlinear regression. The governing function for this network architecture is given in Eq. (3) where I is the input, O is the output, M is the total neurons, W is the weight, and B is the bias. $U = 28$ for the total points in the input pattern while $v = 1$, 2 or 3 for the three damage parameters identified.

$$O_v = \sum_{m=1}^{M} W_{v,m} \mathrm{F}\left(\sum_{u=1}^{U} W_{m,u} I_u + B_m \right) + B_v \qquad (3)$$

The training data consisted of a set of input pattern and corresponding target parameter pairs. Training was supervised with weights and biases adjusted via a resilient backpropagation algorithm [14] by minimizing the mean square error between outputs and targets. This algorithm was suitable to process large networks due to its fast adaptive code and low memory requirements. As there were substantial differences in orders of magnitude among the three damage parameters, these known parameters were scaled in the range [-1,1] for training. Therefore, the test results were also obtained within this scaled range and were required for conversion back into the original magnitudes.

Validation with early stopping [15] was applied during training as a regularization procedure to improve generalization. The size of the validation set consisted of half the training set, which was the accepted solution for adequate verification purposes and fast processing time. Another regularization method conducted was the inclusion of noise into the training patterns [13]. The range of noise levels was initially measured from the experimental signals. Based on the measurement, half the simulated signals for training were added with noise with zero mean and standard deviations that varied between 0.001 and 0.01 before performing the discrete wavelet transform.

A systematic approach [16] was adopted to design the optimum number of neurons in the hidden layer and the size of the training set. The outcome was a neural network with 10 neurons in the hidden layer and a training set size of 4845

patterns that resulted in a validation set size of 2423 patterns. The same architecture and design was maintained throughout the series network processing for consistency while assuming that a network that worked well for a training range would work equally well for a subset of the range.

3 Weight-Range Selection through a Series Network

The concept of a test pattern dependent neural network is based on combined networks [17] by joining conventional neural network processes in a series. The intermediate test results from a neural network can then be used to limit the parameter space for improved generalization in training the subsequent network. The weight-range selection (WRS) is introduced for this purpose to bridge between the networks in series.

3.1 Potential of Weight-Range Selection

Errors calculated from test results obtained from single runs of conventional neural network processes conducted through 50 trials are shown in Fig. 3. The errors presented are for both the experimental and the equivalent simulated test patterns to allow for comparison. Accurate test results observed for simulated patterns with an average error, $<E>$, of 6mm, and standard deviation, σ, of 15mm, verifies the appropriate application of the neural network architecture and design. In comparison, large uncertainties and fluctuations were dominant for testing with the experimental pattern, although the pattern exhibited excellent correlation with simulation in Fig. 2 and Table 3. As the same training, validation and test patterns were used in all the trials, the fluctuations in the results were initiated by random selection of initial weights including biases in Eq. (3). This highlights the important difference in identification results between experiment and simulation from a neural network trained with simulated patterns for the present pattern recognition system.

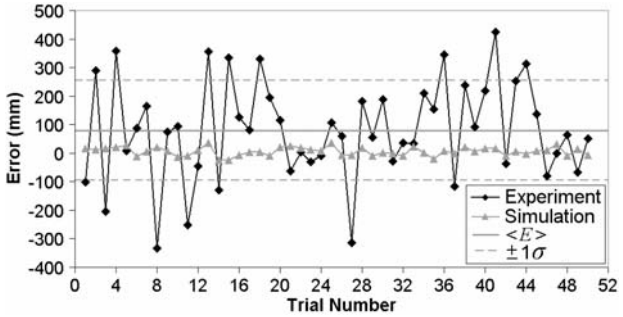

Fig. 3. Errors in DCP for testing the T3 experimental and simulated patterns in 50 trials.

The random initialization of weights is a property of neural networks that results in no unique solution [18]. Training only ensures that for any random initial weights, the function approximated at the end of training gives minimum error with respect to the training data. Even when minimum error is achieved after training for a particular set of initial weights, the trained network might not necessarily give good generalization for the test pattern being identified. A broad variation in regression trends exists with some approximations being more favorable than others in obtaining accurate pattern recognition results from the test pattern. Although subtle discrepancies between experimental and simulated patterns are present, as observed in Fig. 2(b), due to noise and complex wave propagation effects already mentioned in Section 1, this significantly reduces the proportion of regression trends that can map accurately to the experimental patterns.

Table 4. Calculated $<E>$ and σ values for the three damage parameters in beam specimens T1 – T5.

Beam	Damage Parameter	$<E>$ (mm)	σ (mm)
T1	DCP	-7	175
	DD	-0.9	1.5
	DL	53.9	65.5
T2	DCP	16	185
	DD	0.1	1.5
	DL	-47.1	83.1
T3	DCP	79	175
	DD	-0.3	1.5
	DL	-7.3	78.1
T4	DCP	74	193
	DD	-0.2	1.9
	DL	-20.1	72.2
T5	DCP	45	206
	DD	0.0	1.6
	DL	-6.0	71.0

It is thus essential to conduct a reasonable number of trials for training different random initial weights to obtain a more confident measure of the quality of generalization, as performed in Fig. 3. Identifying the test pattern can then be based on the statistics from all the trained neural networks from the trials. According to Fig. 3, the plotted $<E>$ provides a more confident prediction with the actual parameter within $\pm 1\sigma$. $<E>$ and σ values for the other test specimens are tabulated in Table 4. The calculated results in Table 4 also show differences in accuracies among test cases when comparing the

same damage parameters, clearly indicating that the performance of the pattern recognition system is case-specific and test pattern dependent. Thus, application of the WRS test pattern dependent technique in the present damage identification system by narrowing the training range based on the statistics in Table 4 is introduced in the next section as a feasible approach to improve generalization.

3.2 Methodology

The WRS technique functions by reducing the size of the training range using statistics calculated from the test results obtained through a specified number of neural network trials, *K*. Training and validation patterns are then generated randomly within the new parameter space. As the number of training patterns is kept constant, the WRS technique requires the availability of large data sets or data generation.

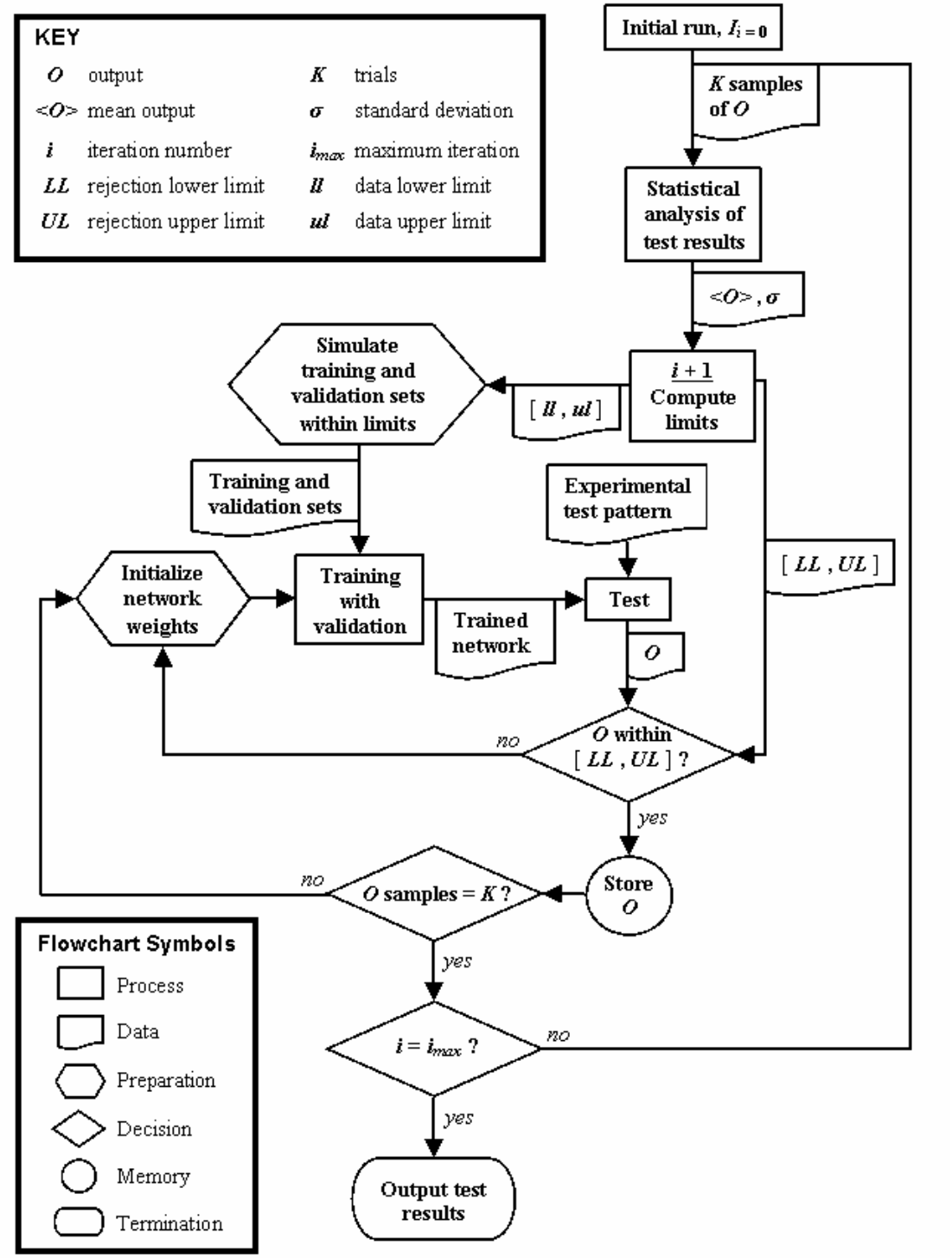

Fig. 4. Flowchart shows the main processes of the weight-range selection (WRS) in a series network.

Training and test then resume but initial weights are restricted to only those that allow the trained network to produce test pattern identification results within the new parameter space. Results that are predicted outside this parameter space are from extrapolation, which are generally considered unreliable [19]. This procedure thus filters out poor initial weights and removes the unreliable results they produce from being considered as a trial.

Obtaining K accepted trials mark the end of the iteration in the series network. Statistical analysis is performed on the test results in the next iteration and the cycle repeats until the maximum number of iterations, I_{max}, is achieved. The statistical analysis procedure is explained in the next section. A flowchart illustrating the integration of the WRS technique into a series network is shown in Fig. 4.

The final outputs via WRS are the product of learning from a training set that is determined from results for the test pattern that is being identified in the first place. This creates a case-specific neural network scheme that uniquely identifies the test pattern that it depends on, naturally turning into a symbiotic system.

The rationale of reducing the size of the training range within the statistical boundaries of the test pattern identification results lies in the likelihood of improving generalization, which can be described by underfitting and overfitting [13]. Underfitting can be minimized, as the function approximated by the neural network for smaller parameter spaces is less complicated without the need to consider trends of patterns outside the space, thus promoting greater accuracy. Overfitting can also be minimized because in a smaller parameter space with the same number of patterns, the amount of interpolations required for regression can be reduced. However, it is important to note that ultimately, the quality of generalization depends on the mapping between inputs and targets, and the sensitivity of that mapping with respect to the test patterns.

The WRS method aims to improve generalization by managing the variation in regression trends through the control of the initial weights. However, the content of the training data can also influence the neural network outputs, which have led to research in network ensembles applying methods like bagging and boosting [17]. These methods can be integrated into the WRS technique and is a subject of further research.

3.3 Statistical Analysis

The statistical analysis introduced extracts the mean output, $<O>$, and the standard deviation, σ, from the K samples of output results, O. These statistical properties are used to calculate the limits of the new training range for data generation, $[ll,ul]$, and the limits of the range to accept O, $[LL,UL]$. Two types of limits are required because $[ll,ul]$ is not equal to $[LL,UL]$ when the actual parameter is located close to the boundaries of the training range. Here, LL or UL is then allowed to be located outside the training range to sustain a balanced spread of the sample results for the correct calculation of the statistics. Extrapolation in this situation is permitted and the results produced outside the training range are considered reliable. This allowance is necessary to enable the detection and characterization of damages located close to the boundaries of the training range.

The expressions and conditions that govern both the required limits for the ith iteration are given in Eq. (4) and Eq. (5). n is a constant that denotes the number of standard deviations. Eq. (4) shows the application of basic statistics to determine the limits of the new training range. This equation can be modified or replaced with more favourable expressions based on more advanced statistics or other mathematical concepts that may better represent the distribution of the samples.

$$[LL_i,UL_i]=[<O>_i-n\sigma_i\ ,<O>_i+n\sigma_i]\quad ;i\neq 0 \tag{4}$$

$$[ll_i,ul_i]=\begin{cases}[ll_0,ul_0] & ;i=0 \text{ OR} \\ & (LL_i<ll_0 \text{ AND } UL_i>ul_0)\\ [LL_i,ul_0] & ;i\neq 0 \text{ AND} \\ & LL_i>ll_0 \text{ AND } UL_i>ul_0\\ [ll_0,UL_i] & ;i\neq 0 \text{ AND} \\ & LL_i<ll_0 \text{ AND } UL_i<ul_0\\ [LL_i,UL_i] & ;i\neq 0 \text{ AND} \\ & LL_i>ll_0 \text{ AND } UL_i<ul_0\end{cases} \tag{5}$$

Selection of n in Eq. (4) can be based on sample distribution of past results for known output parameters of similar neural network tests. If this is not available, the confidence level desired for the new range can be used as a gauge for n. More confident ranges can be achieved by choosing a larger n value. However, n is inversely related to the range reduction rate where large n values can cause the range to converge too slowly to the parameters identified, causing the need for many iterations of the series network and an impractically long processing time.

4 Results and Discussion

Neural network architecture described in Section 2.5 was prepared to identify the damages in the five beam specimens of Table 1. The neural network was integrated into a series network illustrated in the flowchart of Fig. 4. $K = 50$ was selected to obtain an adequate number of samples to represent the distribution of the test results. Statistical analysis was based on Eq. (4) while the limits for the new training and rejection ranges were determined from Eq. (5). $n = 1$ for a confidence interval of 68.3% and a reasonably fast range reduction rate. Based on n and the original damage parameter space sizes given in Table 2, $I_{max} = 3$ was selected to provide sufficient room for improvement in generalization within the series network.

Computations were performed with MATLAB® equipped with the Neural Network Toolbox 4.0.4. The damage identification results for the individual iterations in the series network are plotted as three separate histograms according to the damage parameters in Fig. 5. Table 5 shows the associated percentage change in the results from I_0 to I_3, normalized by the size of the respective original damage parameter space.

According to Fig. 5, the final pattern recognition predictions after three iterations in the series network are on average 2.5%, 7.8% and 23.5% of the original damage parameter space sizes for DCP, DD and DL respectively. DL is clearly less accurate compared to DCP and DD due to the difficulty in quantifying from the training patterns the pulse length, which is the major signal signature that identifies DL. On the other hand, DCP and DD, related to the location and amplitude of the pulses respectively can be more explicitly gauged from the signal and pattern, as shown in Fig. 2.

The WRS technique in the series network provided most benefit for test cases where the damage is poorly recognized initially, notably in DCP of T3, T4 and T5, DD of T1 and T3, and DL of T1 and T2. This observation is supported by the corresponding positive percentage increase in accuracies given in Table 5 with DCP of T3 achieving the best improvement at 13.9%.

Fluctuations in the results among the iterations are also frequently present in the histograms. This is conceived as the prediction tolerance, a property of neural networks caused mainly by changes in the content of the training patterns as well as the random initial weights [13]. The level of tolerance depends on the variation in sensitivity of the regression maps formed from training with the test patterns. A broad range of sensitivity causes a high tolerance level with relatively large changes during the fluctuations, for example in DCP of T2, DD of T2 and T5.

The prediction tolerance affects the performance of the series network. If further improvements in generalization for the parameter being identified cannot be achieved, the results fluctuate within the tolerance range of the perceived prediction in subsequent neural network iterations. This explains the stagnant performance after significant initial improvements in accuracy for subsequent iterations down the series network, most obvious in DCP of T4 and T5, DD of T3 and DL of T1 and T2.

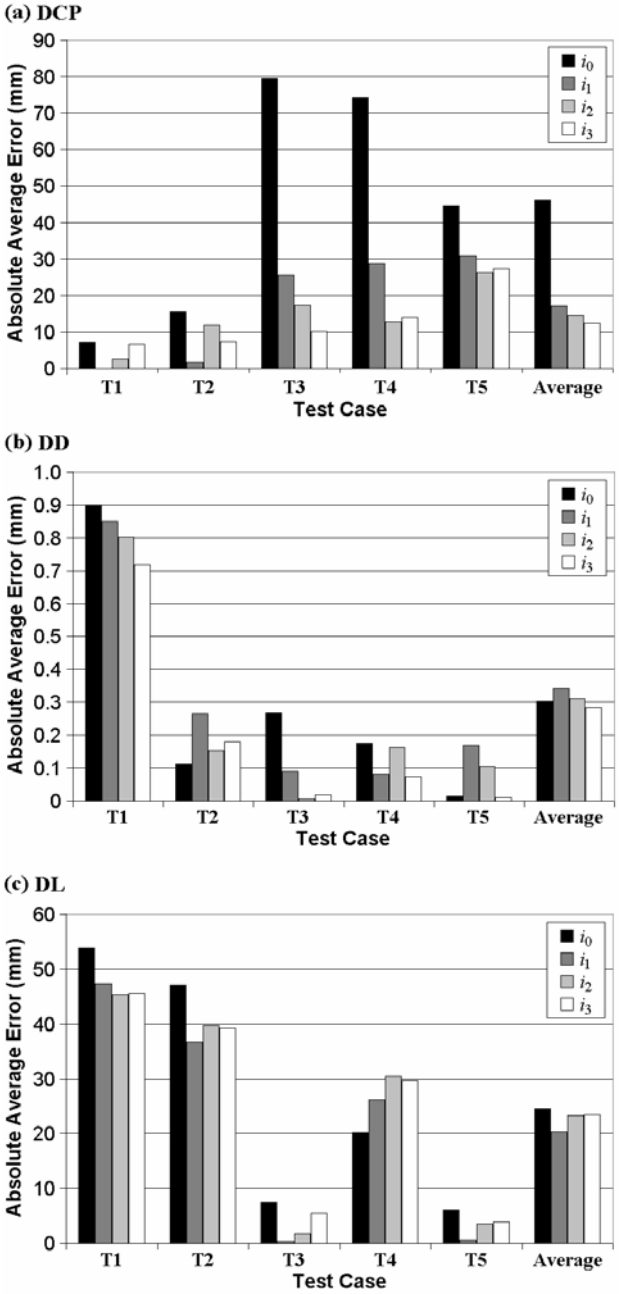

Fig. 5. Damage identification results for the individual iterations in the series network with the WRS technique.

Table 5. Percentage change in the results from I_0 to I_3, normalized by the size of the respective original damage parameters.

Beam	DCP (%)	DD (%)	DL (%)
T1	0.1	6.0	8.3
T2	1.7	-2.3	7.9
T3	13.9	8.3	1.9
T4	12.0	3.4	-9.5
T5	3.4	0.1	2.1

The prediction tolerance can also cause potentially worse accuracies in the final results compared to the initial output in I_0. This is caused by the lack of improvement in generalization with WRS in subsequent iterations after I_0 while the result has fluctuated to a less accurate region within the tolerance range. However, the likelihood of such an event is relatively low as indicated in Table 5 where DD of T2 and DL of T4 are the only two cases that experience this negative impact.

Results for DCP of T3 and DD of T1 in Fig. 5 suggest that further improvement in generalization and thus more accurate predictions can be obtained by running more than the three iterations conducted in this study. However, with range reduction rates at 1σ, these cases have probably arrived at the tolerance range of the perceived prediction where subsequent iterations will bring no significant increase in accuracy.

5 Conclusions

A guided waves damage identification system for beams applying the test pattern dependent WRS technique in a series network has been developed with promising potentials for improving the performance of regression neural networks. Average predictions among five test cases with different fabricated damages after three iterations of the series network were very accurate for DCP and DD at 2.5% and 7.8% of the original parameter space sizes respectively. The WRS technique was able to yield improvement in prediction accuracies up to 13.9% compared to the equivalent single neural network run. It was also found that the prediction tolerance could affect the performance of the WRS technique by fluctuating results within the tolerance range of the perceived prediction, causing no significant increase in accuracy in subsequent neural network iterations.

This new neural network scheme introduced is not restricted to the present damage identification system, as it is designed to function for any pattern recognition problems that contain relatively high uncertainties in predictions due to random initial weights. The WRS technique also encourages further research and development to improve its effectiveness in retrieving the most accurate predictions. The flexibility of the technique allows integration with other training methods like bagging and boosting while modifying or replacing the basic statistical analysis to accommodate more advance mathematical concepts and algorithms is also a possible area of further studies.

6 Acknowledgements

C.K. Liew is grateful for the support received from an International Postgraduate Research Scholarship (IPRS) awarded by the Australian Department of Education Science and Training (DEST), and a UQ Graduate School Scholarship (UQGSS) awarded by the University of Queensland (UQ). The authors would also like to thank Assoc. Prof. David Mee for his advice from a few invaluable discussions.

References:

[1] W.J. Staszewski, C. Boller, and G.R. Tomlinson, *Health Monitoring of Aerospace Structures*, John Wiley & Sons Ltd., 2004.

[2] M. Staudenmann, *Structural Waves in Nondestructive Testing*, Doctor of Technical Sciences Thesis, Institute of Mechanics, Swiss Federal Institute of Technology, 1995.

[3] Z. Su, Y. Lin, and Y. Lu, Guided Lamb Waves for Identification of Damage in Composite Structures: A Review, *Journal of Sound and Vibration*, Vol. 295, 2006, pp. 753-780.

[4] C.K. Liew and M. Veidt, Evaluation of Laminar Defects in Beams using Guided Waves and Pattern Recognition Techniques, *Proceedings of the 1st International Conference on Structural Condition Assessment, Monitoring and Improvement*, 2005, pp. 231-238.

[5] Z. Su, and Y. Lin, An Intelligent Signal Processing and Pattern Recognition Technique for Defect Identification using an Active Sensor Network, *Smart Materials and Structures*, Vol.13, 2004, pp. 957-969.

[6] A. Raghavan and C.E.S Cesnik, Review of Guided-Wave Structural Health Monitoring, *Shock and Vibration Digest*, Vol. 39(2), 2007, pp. 91-114.

[7] C.H. Wang and L.R.F. Rose, Wave Reflection and Transmission in Beams Containing Delamination and Inhomogeneity, *J. Sound and Vibration*, Vol. 264, 2003, pp. 851-872.

[8] C. Yang, L. Ye, Z. Su and M. Bannister, Some Aspects of Numerical Simulation for Lamb Wave Propagation in Composite Laminates, *Comp. Struct.*, Vol. 75, 2006, pp. 267-275.
[9] M.A. Meddick, On Dispersion of Longitudinal Waves in Rectangular Bars, *Journal of Applied Mechanics*, Vol. 34, 1967, pp. 714-717.
[10] K.F. Graff, *Wave Motion in Elastic Solids*, Dover Publication Inc., 1991.
[11] W.B. Fraser, Stress Wave Propagation in Rectangular Bars, *International Journal of Solids Structures*, Vol. 5, 1969, pp. 379-397.
[12] M. Misiti, Y. Misiti, G. Oppenheim and J.M. Poggi, *Wavelet Toolbox User's Guide*, The MathWorks Inc., 2000.
[13] C.M. Bishop, *Neural Networks for Pattern Recognition*, Oxford University Press, 1995.
[14] M. Riedmiller and H. Braun, A Direct Adaptive Method for Faster Backpropagation Learning: The RPROP Algorithm, *Proceedings of the 1993 IEEE International Conference on Neural Networks*, 1993, pp. 586-591.
[15] H. Demuth and M. Beale, *Neural Network Toolbox User's Guide*, The MathWorks Inc., 2004.
[16] C.K. Liew and M. Veidt, Optimization of Neural Network Pattern Recognition Systems for Guided Waves Damage Identification in Beams, *Review of Progress in Quantitative Nondestructive Evaluation 26A*, 2007, pp. 627-634.
[17] A.J.C. Sharkey, *Combining Artificial Neural Nets, Ensemble and Modular Multi-Net Systems*, Springer-Verlag, 1999.
[18] A. Zaknich, *Neural Networks for Intelligent Signal Processing*, World Scientific, 2003.
[19] E. Barnard and L.F.A. Wessels, Extrapolation and Interpolation in Neural Network Classifiers, *IEEE Control Systems Magazine*, Vol. 12, No. 5, 1992, pp. 50-53.